# Compressed Sensing with Interleaving Slow-Time Pulses and Hybrid Sparse Image Reconstruction

*Jabran Akhtar, Børge Torvik and Karl Erik Olsen*

Norwegian Defence Research Establishment (FFI)
Box 25, 2027 Kjeller, Norway
Email: jabran.akhtar@ffi.no, borge.torvik@ffi.no, karl-erik.olsen@ffi.no

***Abstract*— This paper explores a type of hybrid sparse reconstruction technique for modern multifunction task scheduling radars and on following range-Doppler plots. A compressed sensing (CS) framework is devised to emit and then receive interleaved radar pulses in a scarce manner within a coherent processing interval. Sparse reconstruction methods are subsequently employed to regenerate full resolution range-Doppler images. Hybrid reconstructed solutions are finally formed by merging acquired data with sparsely recovered solutions. We show that this is essential for obtaining robust results in the presence of noisy environments and to measure outcomes on equal terms. Real data obtained from an experimental radar observing a Boeing 737 aircraft is employed to demonstrate the practical effectiveness of CS and hybrid sparse reconstruction.**

Keywords: Range-Doppler, Delay-Doppler, slow-time, compressed sensing, sparse reconstruction

## I. Introduction

A pulse-Doppler radar normally operates by transmitting a pulse and performing a matched filtering operation on the incoming delayed and Doppler-shifted pulse echoes; a process which is repeated within a defined coherent processing interval (CPI). A range-Doppler plot may be constructed by executing a Fourier transform over the collected data in slow-time. The emphasis of this work is on extending compressed sensing (CS) and sparse reconstruction techniques [1], [2] to modern multifunction radars. These radars utilize electronically steering arrays and can instantaneously alter the direction where a beam may be pointing. A CS radar in this context may be designed to split the number of pulses available within a CPI between several distinctive directions and ranges. Flexible task scheduling and time splitting, however, results in limited acquired data over various range cells and full high resolution range-Doppler maps can not be composed.

Several papers have successfully demonstrated the capability of CS and sparse reconstruction in a radar context [3], [4], [5], [6], [7]. Many of the presented approaches are based on concepts such as transmission of specific waveforms, irregular sampling in fast-time without matched filtering and simultaneous two-dimensional optimization across both range and velocity. In [7] an alternative design focusing on a less general pulse-to-pulse slow-time sparse pulse emission was proposed and only verified via simulations. Nevertheless, a common trait of all the earlier works is that the sparse solutions found are considered final. The resulting matrix will therefore contain a very large number of zeros and have a characteristical "blue" background in a displayed image. The ability to deal with noise and smaller targets is therefore not always transparent as all signal values below a certain threshold will generally be eliminated alongside the more finer details. This further makes it problematical to compare the exact performance of sparse reconstruction methods with respect to SNR, resolution and so on.

In comparison to [3], [4], [5], [8] in this paper it is not assumed that the radar emits specific modulated pulses or that the sampling is done in a sparse or irregular fashion. We postulate that sampling of incoming waveforms at a given rate is not really a hindrance and rather emphasize emission and thereupon reception of whole pulses in a sparse manner. Further on, each range bin is treated as a separate one-dimensional problem leading to the use of tractable partial Fourier matrices. This allows for a large number of possible targets in the range-Doppler plot with the sparsity constrain only applying on each range bin.

The main contributions of this paper are threefold: 1) A general framework extending and now incorporating full interleaving of pulses is proposed for a CS pulse-Doppler radar. 2) A hybrid sparse reconstruction technique is suggested where the recovered sparse solution is only employed partly to fill in empty data gaps. 3) Real data from an experimental radar setup is used to demonstrate the introduced principles.

## II. Radar system model

We model a type of compressed sensing radar where emission and reception of $N$ pulses takes place during a CPI. At the start of each interval a pulse is emitted at a specific direction. After transmission the radar may start listening for incoming reflections up to a determined range. The radar may also alternate between various interleaving modes and transmit other pulses at different angles. At desired times the radar may switch attention between the various directions listening for arriving echoes; thus only covering specified range regions for distinctive orientations. The procedure will normally follow specific resource manager optimization [9].

Under ideal circumstances, without pulse interleaving and no gaps, the incoming reflected waveform $p(t)$ from a specific

Dette er en postprint-versjon / This is a postprint version.
DOI til publisert versjon / DOI to published version: 10.1109/RADAR.2017.7944161

direction at slow-time $u = 1, 2, ..., N$ can be described by

$$s(t,u) = \sum_n \sigma_n p(t - \Delta_n) e^{j v_{n,u}} + \tilde{w}(t) \quad (1)$$

where $t$ is fast-time, $\sigma_n$ are the reflectivity levels of incoming echoes while $\Delta_n$ is the signal delay associated with each reflector $n$ and $j = \sqrt{-1}$. $\tilde{w}(t)$ is white Gaussian noise and $e^{j v_{n,u}}$ is the experienced Doppler phase shift which for a constant velocity object is typically modeled by

$$v_{n,u} = v_{n,u-1} + \frac{\vartheta_n \, 4\pi f_c}{c \, \text{PRF}}, \quad (2)$$

where $\vartheta_n$ is the radial velocity of target $n$, $f_c$ being the carrier frequency, PRF is the pulse repetition frequency and $c$ is the speed of light [10]. We define $v_{n,0} = 0$. It is assumed that within the burst of $N$ pulses the targets do not vary in amplitude and there is no range walk.

After transmission of each waveform the radar samples any incoming pulse reflections and a matched filtering operation is carried out via the time-reversed and conjugated $p^*(-t)$,

$$Y(t,u) = \sum_n \sigma_n p^*(-t) * p(t - \Delta_n) e^{j v_{n,u}} + w(t) \quad (3)$$

where $*$ prescribes convolution in fast-time. In a practical setting the fast-time parameter will also be discrete, this can explicitly be re-written with range bin as the first parameter when all available data is referred by a single matrix

$$\mathbf{Y}(r,u) = Y(r \, \Delta t, u) \; \in \mathbb{C}^{N \times R}, \; r = 1, 2, ...., R, \quad (4)$$

given $\Delta t$ as the time-resolution of the radar.

For further processing each column of $\mathbf{Y}(r,u)$ indicated by $\mathbf{y}_r(u)$, is multiplied element-wise by a windowing function $\mathbf{w}(u) \; \in \mathbb{C}^{N \times 1}$. Performing a Fourier transformation, with respect to slow-time, results in a range-Doppler representation $\mathbf{d}_r(\omega)$:

$$\mathbf{d}_r(\omega) = \mathbf{F} \; \mathbf{w}(u) \mathbf{y}_r(u) \; \in \mathbb{C}^{N \times 1}. \quad (5)$$

$\mathbf{F}$ is the discrete Fourier matrix of size $N \times N$, $\mathbf{F}_{k,l} = \exp(-j 2\pi kl/N)$. The main components forming the contour are consistent phase shifts originating from (2). Assembling together the Doppler profiles in a matrix column-wise results in a range-Doppler map $\mathbf{D}(r,\omega) \in \mathbb{C}^{N \times R}$. Targets with a steady velocity within the CPI will after Fourier processing appear concentrated in Doppler.

### A. Sparse reconstruction

We next assume that the radar operates in a sparse pulse emission mode, as described earlier, and only emits $K < N$ pulses towards a set direction within a dwell. In addition to that, the receiver may operate in an interleaving mode thus the number of slow-time samples available at a particular range bin $\hat{r}$ is specified by $K_{\hat{r}} \leq K$. In the following we drop the subscript $\hat{r}$ for simplicity, implicitly assuming that the process is independently repeated across all range bin.

The limited available data is denoted by $\tilde{\mathbf{Y}}(r,\tilde{u})$ and the column specifying range bin $\hat{r}$ given by $\tilde{\mathbf{y}}(\tilde{u})_{\hat{r}} \in \mathbb{C}^{K_{\hat{r}} \times 1}$, $\tilde{u} = 1, 2, ..., K_{\hat{r}}$. The slow-time positions where data is collected, perhaps arbitrary within the CPI of $N$ pulses, is designated by the set $D_{\hat{r}}$. With uneven measurements the target Doppler model (2) will follow a discontinuous form

$$v_{n,\tilde{u}} = v_{n,\tilde{u}-1} + k_{\hat{r}}(\tilde{u}) \frac{\vartheta_n \, 4\pi f_c}{c \, \text{PRF}}, \quad (6)$$

where any phase discrepancies can be considered describable by a function $k_{\hat{r}}(\tilde{u}) \in \mathbb{N}$. Empty gaps and incoherent data lead to spectral leakage and lower integration gain.

The sparse reconstruction solution to the above problem is an attempt to assemble an extended range-Doppler profile and to retain a high resolution in slow-time. The ideal solution should inter- and / or extrapolate to expand (6) into a form of (2) with coherent phases across slow-time as only this would lead to full focusing of each individual target in Doppler. As the overall profile is assumed to only contain a few targets the solution will be the one that maximizes sparsity in frequency. We define $L$ to indicate the number of desired output entries in slow-time with $L \geq N$, an $L > N$ signifying extrapolation. The reconstructed profile for range bin $\hat{r}$ in slow-time is denoted by $\hat{\mathbf{y}}_{\hat{r}}(\hat{u}) \in \mathbb{C}^{L \times 1}$, $\hat{u} = 1, ..., L$ and the relationship to range-Doppler map is as previously governed by

$$\hat{\mathbf{d}}_{\hat{r}}(\hat{\omega}) = \hat{\mathbf{F}} \; \hat{\mathbf{w}}_{\hat{r}}(\hat{u}) \hat{\mathbf{y}}_{\hat{r}}(\hat{u}) \; \in \mathbb{C}^{L \times 1} \quad (7)$$

where $\hat{\mathbf{F}}$ is an $L \times L$ Fourier matrix. We further define a binary selection matrix $\mathbf{M}_{\hat{r}} \in \mathbb{B}^{K_{\hat{r}} \times L}$ by taking an $L \times L$ identity matrix $\mathbf{I}_{L \times L}$ and removing respective rows for which no collected data is available. We specify this as

$$\mathbf{M}_{\hat{r}} = H_{D \, \hat{r}}(\mathbf{I}_{L \times L}) \quad (8)$$

where the function $H_{D \, \hat{r}}$ only preserves the rows of the given matrix as specified by the set $D_{\hat{r}}$. The purpose of the selection matrix is to allow for extraction of values from positions where slow-time data has been accumulated. We further form $\bar{\mathbf{w}}_{\hat{r}}(\tilde{u})$ by selecting a windowing function of $L$ entries, $\hat{\mathbf{w}}(\hat{u}) \in \mathbb{C}^{L \times 1}$, and truncating it:

$$\bar{\mathbf{w}}_{\hat{r}}(\tilde{u}) = \mathbf{M}_{\hat{r}} \hat{\mathbf{w}}(\hat{u}) \; \in \mathbb{C}^{K_{\hat{r}} \times 1}. \quad (9)$$

The reconstructed profile should agree with measured data where available, which inclusive tapering, can be expressed as

$$(\mathbf{M}_{\hat{r}} \hat{\mathbf{y}}_{\hat{r}})(\tilde{u}) = \tilde{\mathbf{y}}_{\hat{r}}(\tilde{u}). \quad (10)$$

To simplify, the index terms are only given for the final product. With windowing functions incorporated the requirement becomes

$$\mathbf{M}_{\hat{r}}(\hat{\mathbf{w}} \hat{\mathbf{y}}_{\hat{r}}) \; (\tilde{u}) = (\mathbf{M}_{\hat{r}} \hat{\mathbf{w}}) \tilde{\mathbf{y}}_{\hat{r}} \; (\tilde{u}), \quad (11)$$

$$\text{or} \qquad \hat{\mathbf{F}}_{M,_{\hat{r}}} \hat{\mathbf{d}}_{\hat{r}} \; (\hat{\omega}) = \bar{\mathbf{w}}_{\hat{r}} \tilde{\mathbf{y}}_{\hat{r}} \; (\tilde{u}), \quad (12)$$

given the partial inverse Fourier matrix $\hat{\mathbf{F}}_{M,_{\hat{r}}} = \mathbf{M}_{\hat{r}} \hat{\mathbf{F}}^* \; \in \mathbb{C}^{K_{\hat{r}} \times L}$.

The objective of the reconstruction procedure is therefore to determine a sparse Doppler profile $\hat{\mathbf{D}}_{\hat{r}}(\hat{\omega})$ consisting of $L$ Doppler samples while concurring with the observations. This can under convex relaxation be set up as:

$$\hat{\mathbf{d}}_{\hat{r}}(\hat{\omega}) = \arg\min ||\dot{\mathbf{d}}_{\hat{r}}(\hat{\omega})||_1 \quad (13)$$

$$s.t. \quad || \; \hat{\mathbf{F}}_{M,_{\hat{r}}} \; \dot{\mathbf{d}}_{\hat{r}}(\hat{\omega}) - \bar{\mathbf{w}}_{\hat{r}}(\tilde{u}) \; \tilde{\mathbf{y}}_{\hat{r}}(\tilde{u}) \; ||_2 \leq \varepsilon \quad (14)$$

Dette er en postprint-versjon / This is a postprint version.
DOI til publisert versjon / DOI to published version: 10.1109/RADAR.2017.7944161

where $\varepsilon$ is acceptable error and $||\ ||_1$ indicates the $L_1$ norm. Finding an independent solution over all ranges $\hat{r} = 1, 2, ...., R$ results in a full range-Doppler map matrix $\hat{\mathbf{D}}(r, \hat{\omega}) \in \mathbb{C}^{L \times R}$ where any missing data would effectively have been inter- or extrapolated. The bin resolution of $\hat{\omega}$ in (13) is now conditioned by $L$, $\Delta\hat{\omega} = \frac{2\pi}{L}$. We remark that in contrast to previous works, among other things, the Fourier matrix is now in principle distinct for each range bin. This flexibility provides opportunities to a pulse interleaving radar as it may increase the number of measurements at ranges of interest to achieve greater robustness in e.g. non-sparse regions due to multiple targets or clutter.

### *B. Hybrid reconstruction*

The sparse solution of $\hat{\mathbf{D}}(r, \hat{\omega})$ can be effective as is, however, it also has several drawbacks. One such disadvantage is that a sparse solution can be seen as indirectly performing a detection procedure which is not always desirable. Secondly, a low figure for $\varepsilon$ will force noise to remain in place thus not yielding clear focusing and enhancement of targets, while a larger threshold can make more sensitive and faint target disappear. This paper therefore proposes a merger of the sparse solution with real measurements where available. At slow-time and range placements without available measurements, results from the sparse solution are utilized otherwise the original data is retained; or alternatively linearly combined with the sparse solution. One significant advantage of this is that $\varepsilon$ can be set to much lower values as a highly sparse image on its own is not sought. Traditional classification, detection and comparison procedures may thereupon be applied on the hybrid reconstructed range-Doppler map $\mathbf{R}_{Hyb}\,(r, \hat{\omega})$. Among other usages, the sparse reconstruction process may be repeated across the Doppler domain on the hybrid image to improve range resolution.

The hybrid range-Doppler map is formed by transforming the sparse range-Doppler solution back to slow-time,

$$\hat{\mathbf{Y}}_S(r, \hat{u}) = \hat{\mathbf{F}}^* \hat{\mathbf{D}}(r, \hat{\omega}) \in \mathbb{C}^{L \times R} \tag{15}$$

where $\hat{\mathbf{F}}^* \in \mathbb{C}^{L \times L}$ is the inverse Fourier matrix. The reconstructed data $\hat{\mathbf{Y}}(r, \hat{u})$ is in time domain infused with collected measurements after tapering

$$\mathbf{Y}_{Hyb}(r, \hat{u}) = \begin{cases} \alpha \bar{\mathbf{w}} \tilde{\mathbf{Y}}(r, \tilde{u}) + \sqrt{(1-\alpha^2)} \hat{\mathbf{Y}}_S(r, \hat{u}), & (r, \hat{u}) \in D \\ \hat{\mathbf{Y}}_S(r, \hat{u}), & (r, \hat{u}) \notin D \end{cases} \tag{16}$$

where $(r, \hat{u}) \in D$ indicates that measured data at given range and slow-time is available. A Fourier transform across slow-time constructs the final hybrid range-Doppler map:

$$\mathbf{R}_{Hyb}\,(r, \hat{\omega}) = \hat{\mathbf{F}}\ \mathbf{Y}_{Hyb}(r, \hat{u}) \in \mathbb{C}^{L \times R}. \tag{17}$$

$0 \leq \alpha \leq 1$ may be chosen to weight the solutions accordingly. In the case of a sparse scene where one is primarily interested in detections more emphasis may be placed on the sparse solution, i.e. $\alpha$ close to zero. On the other hand, to preserve the finer details and obtain a solution resembling a full measured set $\alpha$ may be stipulated to a greater value.

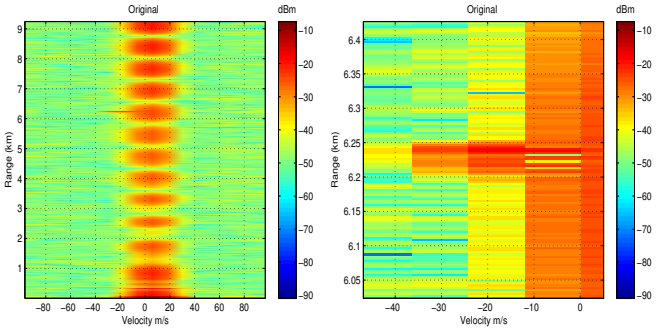


(a) Full (b) Zoomed in, PSNR=28.04dB

Fig. 1: Original R-D map with 16 pulses

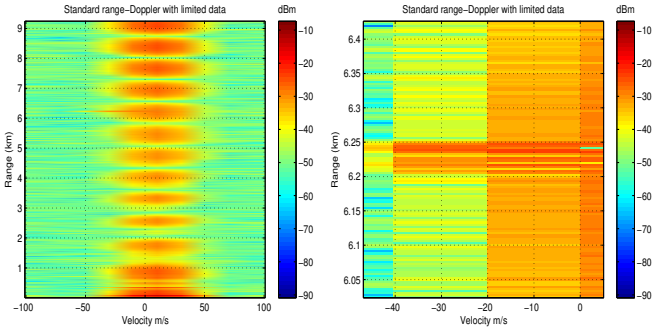


(a) Full (b) Zoomed in, PSNR=24.59dB

Fig. 2: Standard R-D map from limited data (40% reduction)

## III. Trials with an experimental radar

In order to evaluate the practicability of CS and hybrid reconstruction methods data accumulated from an experimental radar was put to use. The S-band radar was aimed at a Boeing 737 flying at a distance of 6.2km. The system was operating at 3.3 GHz with a bandwidth of 50MHz, LFM pulses with horizontal polarization and PRF of 4kHz. The maximum range being approximately $R = 10$km and the radar was managed with adjustable smooth movements to integrate pulses over a longer time frame.

We consider 4 different interleaving transmission and reception strategies for each pulse: $S1$) The radar emits and listens for the full range $[0, R]$. $S2$) The radar has its attention elsewhere and no data is collected with respect to this direction. $S3$) radar emits but listens only covering the range $[0, R/2]$, $S4$) radar transmits though listens only for the range $[R/2, R]$.

### *A. 16 pulses*

We initially examine a burst consisting of the first 16 pulses and figure 1 shows the original full-data range-Doppler plot with the Blackman window. There is significant unfiltered ground clutter and the resolution is not sufficient to fully separate the aircraft from the clutter. This deteriorates further with CS data acquisition (figure 2) where we assume only $S1 = 10$ full-range measurements, $S2 = 4$, while mode S3 and S4 occur 2 times each. The gaps are placed randomly within the CPI. This gives an overall data reduction of $40\%$.

Dette er en postprint-versjon / This is a postprint version.
DOI til publisert versjon / DOI to published version: 10.1109/RADAR.2017.7944161

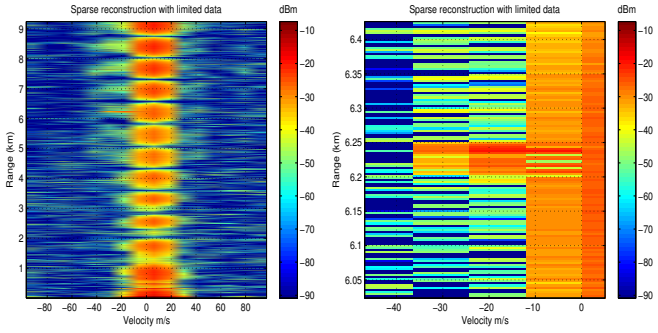


(a) Full (b) Zoomed in

Fig. 3: Sparse reconstruction from limited data

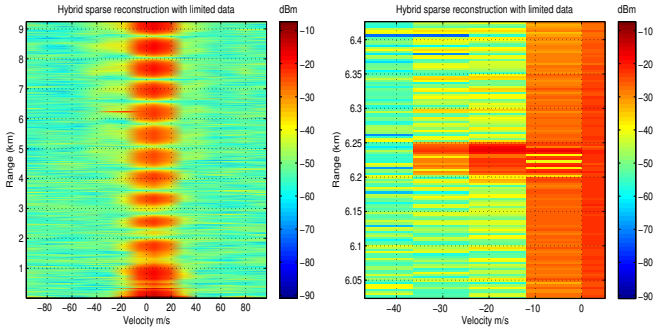


(a) Full (b) Zoomed in, PSNR=31.66dB

Fig. 4: Hybrid reconstruction from limited data, $\alpha = \frac{1}{\sqrt{2}}$

For reconstruction $\varepsilon = 2\hat{\sigma}$ is set for the first simulations, i.e. twice the estimated noise level, alongside $L = 16$. We remark that this is very low level thresholding and a significant amount of noise is aspired retained. The pure $L_1$ solution from (13) and (14) can be seen in figure 3 which is therefore definitely not sparse. Employing the proposed hybrid reconstruction scheme (17) generates noteworthy more practical and traditional looking image in figure 4 amidst $\alpha = \frac{1}{\sqrt{2}}$.

Figure 5 displays hybrid sparse reconstruction with $L = 32$ where an extrapolation of 8 slow-times values is conditioned on both edges, practicing the same reduced data set. The target is now clearly distinguishable from the clutter and is much more localized in velocity. Extrapolation generally contributes with degrees of freedom augmenting the results.

### *B. 400 pulses*

For further analysis the full collected set consisting of 400 pulses is taken advantage of. Out of 400, data reduction was carried out by 50% by selecting $S1 = S2 = S3 = S4 = 100$ randomly within the set. This can be viewed as a radar pointing at a fixed target and compensating for any movements while still simultaneously searching in other directions.

Longer integration times provide with higher resolution as can be seen in the full resolution full data image of figure 7. The next figure 8 is the standard range-Doppler image but

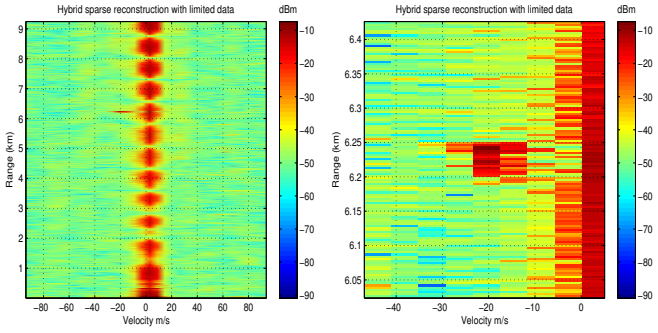


(a) Full (b) Zoomed in, PSNR=38.55dB

Fig. 5: Hybrid reconstruction with extrapolation from limited data

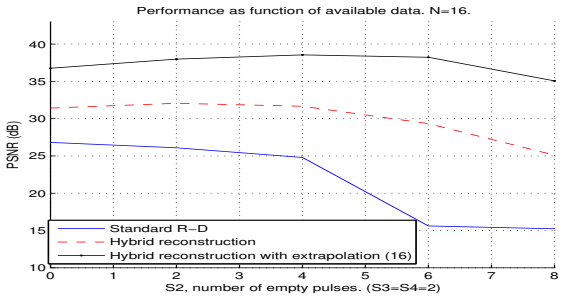


Fig. 6: Performance vs data, $N = 16$, $\alpha = \frac{1}{\sqrt{2}}$.

constructed from the reduced data set showing considerable spectrum leakage.

Figure 9 demonstrates the image regeneration process via sparse reconstruction with an extrapolation of 50 samples on each side bringing forth $L = 500$ output bins in slow-time. The sparse solution itself is confined by the noise threshold level yielding substantial speckle even though the target stands out clear and unambiguous. The hybrid technique, with $\alpha = 1$ shown in figure 10, manages to preserve the refocusing of the target from the sparse image while simultaneously retaining the more traditional properties of a range-Doppler map. The image may be applied in any conventional context.

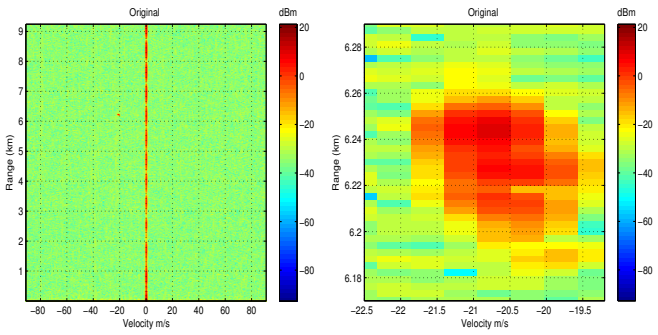


(a) Full (b) Zoomed in, PSNR=41.95dB

Fig. 7: Original R-D map with 400 pulses

Dette er en postprint-versjon / This is a postprint version.
DOI til publisert versjon / DOI to published version: 10.1109/RADAR.2017.7944161

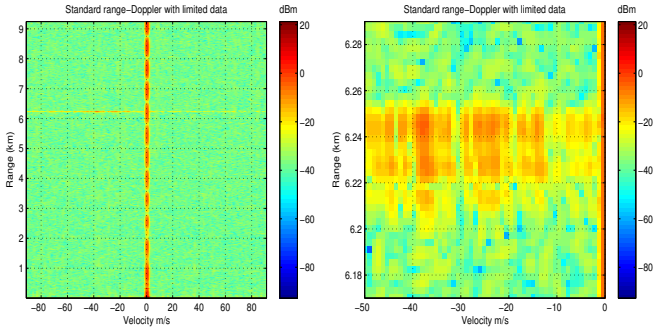


(a) Full (b) Zoomed in, PSNR=23.7dB

Fig. 8: Standard R-D map from limited data (50% reduction)

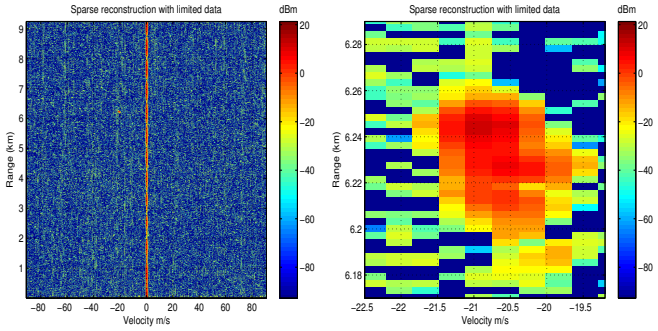


(a) Full (b) Zoomed in

Fig. 9: Sparse reconstruction from limited data

How the peak target SNR varies with different number of empty gaps (S2) is established in figures 6 and 11 for hybrid reconstruction. It is notable that the PSNR can be sustained with reasonably few pulses, the major issue instead being Doppler ambiguities, which arise with limited data and can not be corrected by sparse regeneration. Gaps in data can to some extent also improve hybrid sparse reconstruction techniques as vacant positions provide degrees of freedom, which can be capitalized to narrow down the location in Doppler space.

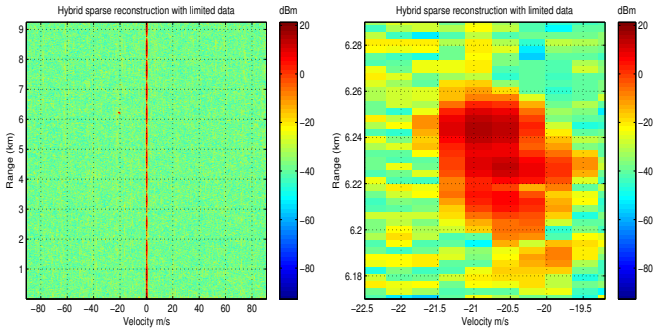


(a) Full (b) Zoomed in, PSNR=46.74

Fig. 10: Hybrid reconstruction from limited data, $\alpha = 1$

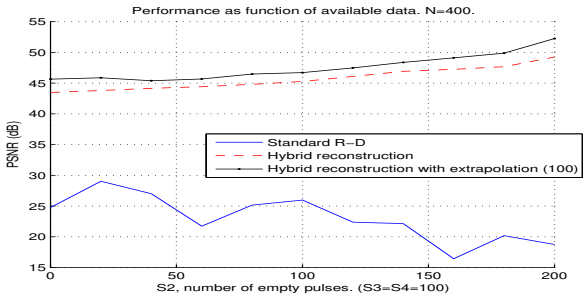


Fig. 11: Performance vs data, $N = 400$, $\alpha = \frac{1}{\sqrt{2}}$.

## IV. Conclusion

Radar systems often rely on range-Doppler maps to detect targets and this work put forward a hybrid sparse reconstruction techniques for their formation. It was shown that through task scheduling and pulse interleaving a radar may reduce the amount of data collected for individual range cells and still manage to effectively regenerate missing data. Hybrid reconstruction permits low threshold values for sparse reconstruction and preservation of the more fine details. Real data collected from an experimental radar aimed at a 737 aircraft was used to demonstrate the various principles.

## References

[1] E. Candès, J. Romberg, and T. Tao, "Stable signal receovery from incomplete and inaccurate measurments," *Communication in Pure and Applied Mathematics*, vol. 59, pp. 1207–1223, 2006.

[2] L. C. Potter, E. Ertin, J. T. Parker, and M. Cetin, "Sparsity and compressed sensing in radar imaging," *Proceedings of the IEEE*, vol. 98, no. 6, pp. 1006–1020, 2010.

[3] M. A. Herman and T. Strohmer, "High-resolution radar via compressed sensing," *IEEE Trans. Signal Processing*, vol. 57, no. 6, pp. 2275–2284, June 2009.

[4] B. Pollock and N. A. Goodman, "Detection performance of compressively sampled radar signals," in *IEEE Radar Conference*, 2011, pp. 1117–1122.

[5] M. M. Hyder and K. Mahata, "Range-doppler imaging via sparse representation," in *IEEE Radar Conference*, 2011, pp. 486–491.

[6] S. Tomei, A. Bacci, E. Giusti, M. Martorella, and F. Berizzi, "Compressive sensing-based inverse synthetic radar imaging imaging from incomplete data," *IET Radar, Sonar & Navigation*, vol. 10, no. 2, pp. 386–397, Feb. 2016.

[7] J.Akhtar and K. E. Olsen, "Formation of range-doppler maps based on sparse reconstruction," *IEEE Sensors Journal*, vol. 16, no. 15, pp. 5921–5926, Aug. 2016.

[8] T. Xing, W. Roberts, L. Jian, and P. Stoica, "Range-doppler imaging via a train of probing pulses," *IEEE Trans. Signal Processing*, vol. 57, no. 3, pp. 1084–1097, March 2009.

[9] H. S. Mir and A. Guitouni, "Variable dwell time task scheduling for multifunction radar," *IEEE Transactions on Automation Science and Engineering*, vol. 11, no. 2, pp. 463–472, April 2014.

[10] W. L. Melvin and J. A. S. (Eds.), *Principles of Modern Radar*. SciTech Publishing, 2013.

Dette er en postprint-versjon / This is a postprint version.
DOI til publisert versjon / DOI to published version: 10.1109/RADAR.2017.7944161